Ferroelectrics, 341:21–28, 2006
Copyright © Taylor & Francis Group, LLC
ISSN: 0015-0193 print / 1563-5112 online
DOI: 10.1080/00150190600889320

Scanning Electrooptic Microscopy of the Relaxor Materials

O. TIKHOMIROV,[1,2,*] M. LABARDI,[1] C. ASCOLI,[3]
AND M. ALLEGRINI[1,3]

[1]polyLab CNR-INFM, Largo Bruno Pontecorvo 3, 56127 Pisa, Italy
[2]Institute of Solid State Physics, Chernogolovka, Moscow region 142432, Russia
[3]Dipartimento di Fisica "Enrico Fermi", Università di Pisa, Largo Bruno Pontecorvo 3, 56127 Pisa, Italy

Scanning electrooptic microscopy provides optical imaging of surface ferroelectric polarization patterns by measuring modulation of the output optical signal induced by a sinusoidal electric field. Ferroelectric single crystals and inhomogeneous phase transitions in ferroelectric thin films were investigated by this technique. Here we report investigation of the domain structure in relaxor materials. We have observed formation and evolution of microscopic domains under the action of a dc bias electric field. Furthermore, the local electrooptic switching loops have been measured with sub-micron resolution. Features of electrooptic imaging in ceramic samples are also discussed.

Keywords Scanning microscopy; electrooptic; relaxors; domain structure

Optical microscopy, being for decades a tool of choice to investigate ferroelectric domain structure, suffers lack of direct coupling between ferroelectric polarization and measured parameters. Birefringence, used generally to distinct ferroelectric domains, is an even effect and gives no contrast between antiparallel domains in many important cases. To overcome this obstacle the use of a modulation principle can be decisive. Though artificial electrooptic contrast between domains induced by a probe electric field is known for a long time [1], its effective use became possible only recently with general development of scanning techniques [2]. Scanning confocal or near-field optical microscopy with electrooptic modulation has been applied effectively to visualize the domain structure in classical ferroelectric crystals like $BaTiO_3$ and $LiNbO_3$, or TGS [3–5] and in ferroelectric thin films [2, 6, 7], to measure local tuning loops [2, 8, 9], and to investigate local phase transitions [8, 9]. This paper is devoted to investigation of the domain structure and its evolution in another important class of electrically ordered materials – relaxor crystals and ceramics.

The experimental setup is similar to the prototype described in [3]. The scanning electrooptic microscope (SEOM) has been constructed using the confocal principle in reflection mode. A high numerical aperture (NA = 0.8) Nikon 50x objective is filled by light of a 633 nm laser passed through a beamsplitter, a spatial filter, and a beam expander. The raster scanning is performed by a perpendicular pair of galvanometric mirrors placed before the

---

Received November 15, 2005; in final form May 24, 2006.
*Corresponding author. E-mail: tikhom@df.unipi.it

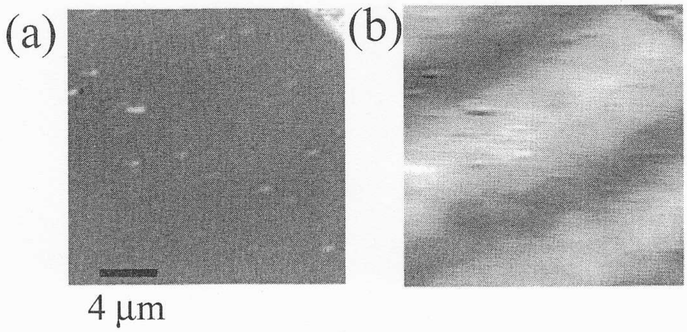

Figure 1. Optical (a) and electrooptic (b) images of the domain structure in a barium titanate single crystal.

objective. The light reflected from the crystal surface passes back through the objective and spatial filter to be registered by a high frequency Nirvana photodetector. Both *ac* and *dc* electric fields can be simultaneously applied to the crystal by specially designed high voltage amplifier. Scanning and data acquisition are managed with a commercial Burleigh AFM controller. Both optical (*dc* signal) and electrooptic (in-phase *ac* component from a lock-in demodulator) pictures are acquired during the same scan. The optical testing of the microscope has been performed with a commercial square metal mesh for transmission electron microscopy; spatial resolution measured at a sharp edge is about 0.55 microns.

Figure 1 illustrates the performance of SEOM using a test sample of tetragonal barium titanate. Pairs of stripe electrodes with spacing of about 0.15-0.3 μm have been painted on the crystal surface with a silver paste at arbitrary angles to the crystallographic axes and powered with the *ac* voltage (10 V, 16 kHz). The laser spot is scanned across the area between the electrodes. The optical image corresponding to the spatial map of the *dc* signal from the photodetector is shown in Fig. 1a. No domain structure is seen in this optical image, and the only visible inhomogeneities are various surface imperfections. The electrooptic image corresponding to the spatial distribution of the in-phase *ac* signal is shown in Fig. 1b. Distinct regular stripe domains can be seen in this image due to opposite sign of their electrooptic response. Bright stripes correspond to in-phase intensity modulation, while electrooptic signal in dark areas has the phase shift of 180^o with respect to excitation. Note that the non-ferroelectric features on the surface are much less visible in the electrooptic picture.

We have studied spatial distribution of ferroelectric polarization in two model relaxor materials, namely, $(1-x)Pb(Mg_{1/3}Nb_{2/3})O_3 - xPbTiO_3$ (PMN-PT) crystals with composition $x = 0.25$, and $Pb(Zr,Ti)O_3$ ceramics (60% Zr) doped with La (7%) and Nb (PLZTN). The relaxor materials, widely studied for decades due to their outstanding dielectric and piezoelectric properties, are expected to contain tiny nanoscopic domains or clusters capable to develop into larger microscopic domains with cooling or with application of a sufficiently high electric field. While observation of nanoscopic domains in the relaxor state with SEOM needs high resolution near-field equipment and is still to be performed, a microscopic stage of the domains evolution during transition into ferroelectric phase is attainable with diffraction-limited confocal SEOM [10].

The electrooptic image of the PMN-PT crystal before any electric treatment shows full absence of any macroscopic domain structure (Fig. 2a); in other words, the *ac* signal is null at any point. This result correlates with the earlier piezoelectric force microscopy observations

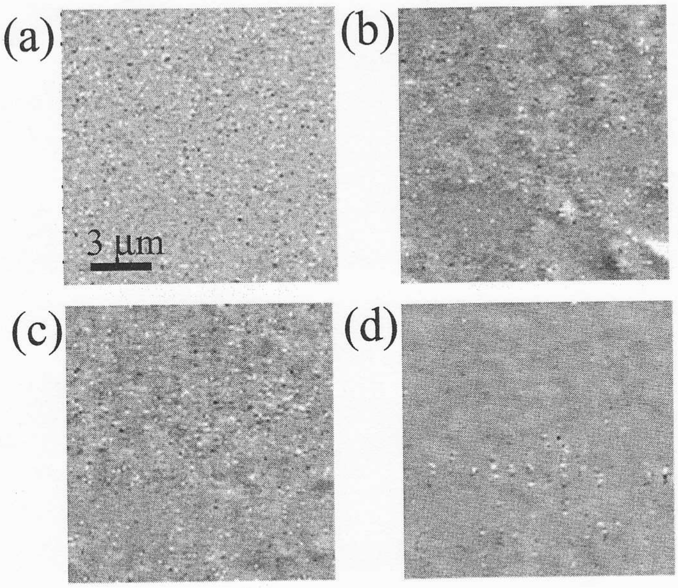

Figure 2. Electrooptic images of a ⟨001⟩ oriented PMN-PT crystal (a) before application of a *dc* bias field; (b) in presence of a *dc* voltage of −50 V; (c) +50 V; (d) 0 V.

of PMN-PT of similar composition, where only separate nanoscopic domains much smaller than the optical wavelength were found [11]. Averaging through the diffraction-limited resolution area cancels out possible contributions to the electrooptic signal from separate nanodomains.

We have observed, nevertheless, that application of moderate *dc* fields induces irreversible formation of microscopic, electrooptically active regions throughout the crystal. Figures 2b–d show the electrooptic pictures after application and variation of the *dc* bias voltage producing an in-plane electric field on the ⟨001⟩ surface. Numerous regions of both positive (bright areas) and negative (dark spots) electrooptic response can be seen, as well as areas with low or null electrooptic response. As known from previous SEOM experience, such regions can correspond either to local paraelectric state or to special direction of ferroelectric polarization [8, 9]. Some of the areas in the electrooptic image can be linked to corresponding structural features seen in the optical image, too. However, most ferroelectric domains, well resolved in the electrooptic mode of observation, have completely similar optical properties, so that they are not visible in the *dc* picture. The induced ferroelectric domains are stable enough, and only small part of them change their shape or size during variation of the bias voltage from –100 to 100 Volts and back. The electrooptic contrast, however, is essentially weaker at lower bias field.

The behavior of the local ferroelectric polarization, described above, has been obtained for a ⟨001⟩ crystal plate. A different sample orientation, namely, plate normal to the ⟨111⟩ pseudocubic axis, shows qualitatively similar electrooptic response: no *ac* signal has been observed from the virgin crystal, while application of the electric *dc* bias field induces stable, distinct electrooptic domain structure. The shape of the domains in this case is a little bit different comparing to ⟨001⟩ samples, featuring elongated domains, often adjacent to similar stripe of opposite sign. This is visible in Fig. 3 that illustrates the changes of the domain structure revealed in *ac* mode for the ⟨111⟩ plate during application and variation of

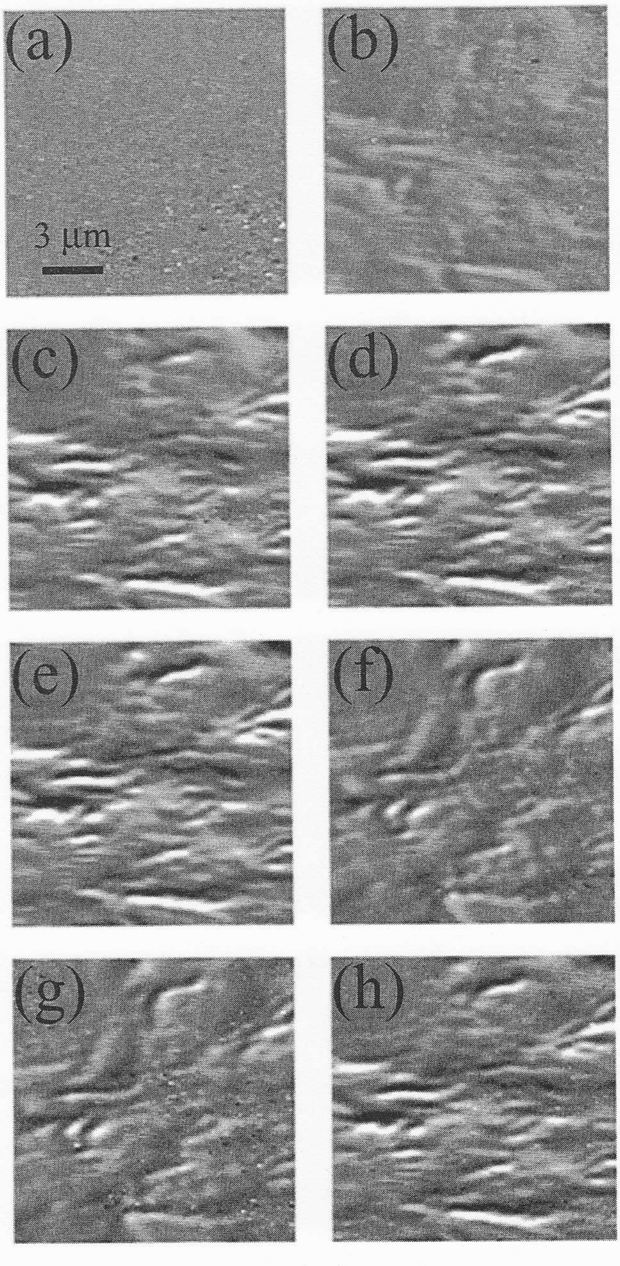

Figure 3. Evolution of the domain structure in a ⟨111⟩ oriented PMN-PT crystal during application and variation of the external *dc* bias voltage: (a) +35 V, (b) +70 V, (c) +100 V, (d) +70 V, (e) 0 V, (f) −35 V, (g) +35 V, (h) +100 V.

the external *dc* bias field. There is no electrooptic response from an as-grown sample even when a low bias voltage is applied (Fig. 3a). The domain structure begins to arise starting from some critical voltage (Fig. 3b) and becomes stable in a higher field (Fig. 3c). Stability of the domain pattern is proved by decreasing the bias voltage back to its previous value (Fig. 3d) and further to zero (Fig. 3e). Reversal of the field sign results in minor changes of this domain structure, mainly in orientation of the stripe domains and overall decrease of the electrooptic contrast (Fig. 3f). This new structure remains approximately unchanged down to –100 Volts and back to positive values (Fig. 3g), where the pattern "written" by high positive voltage reappears (Fig. 3h).

The electrooptic response produced by ferroelectric domain of a certain orientation can be determined considering the electrooptic tensor [3]. The PMN-PT with composition $x = 0.25$ is placed near the boundary between the (macroscopically) pseudocubic $m3m$ phase, giving no linear electrooptic effect, and the rhombohedral ferroelectric and electrooptic $3m$ phase. The latter group is the same as for lithium niobate already studied with SEOM. However, numerical analysis performed in Ref. [3] can not be applied to PMN-PT directly. First, electrooptic constants of PMN-PT are expected to be much different from those of $LiNbO_3$; only mixed "effective" constants have been obtained for several compositions [12]. Second, the simplified two-dimensional analysis [3] is valid only for crystal plates containing the ferroelectric axis in its plane, that is, in our case, for $\langle 110\rangle$ or $\langle 112\rangle$ samples. For other orientations, including our $\langle 001\rangle$ and $\langle 111\rangle$ plates, the quantitative analysis becomes three-dimensional. Qualitative explanation, however, can be given for both observed electrooptic contrast and switching behavior.

Both $\langle 001\rangle$ and $\langle 111\rangle$ samples can bear ferroelectric polarization at some angle to the surface only. The surface in-plane electric field, used in our experiments for both inducing ferroelectric polarization and its visualization through linear electrooptic effect, affects mainly the in-plane component of polarization. It is the value of this angle which provides a difference between $\langle 001\rangle$ and $\langle 111\rangle$ cases. There are eight possible directions of ferroelectric polarization having the same angle with a $\langle 001\rangle$ plane; their in-plane components differ by angles 90° or 180° between them. The out-of-plane component of polarization is large, but not sensitive to the field. The in-plane electric field applied at an arbitrary angle will affect one pair of domains more than the other one (like for mixed 90°/180° domain structure in tetragonal ferroelectrics) making the whole domain pattern "harder". Combined with a relatively small driving field component, we can expect weak response to switching field in $\langle 001\rangle$ samples as observed. As for the electrooptic signal, the large out-of-plane ferroelectric component should have finite, but rather small contrast in presence of an in-plane field, similar to out-of-plane regions in thin films [9].

The eight directions of ferroelectric polarization in the $\langle 111\rangle$ sample are not equivalent: there is one pair normal to the surface (not affected by the in-plane field) and six other directions lying very close to the surface plane with 60° symmetry. The in-plane switching between them is much easier comparing to the previous case. The electrooptic contrast in this configuration is high (and its tuning is asymmetric), similar to in-plane domains in ferroelectric films [9]. This is also in good agreement with our experimental data (Fig. 3).

It is clear from Fig. 3 that the kinetics of the so-formed domain structure during the "switching cycle" is highly asymmetric. The principal reason is, of course, the presence of a high bias field during nucleation and growth of the domains. This field destroys the initial "nanoscopic" state and induces "shifted" configuration of ferroelectric polarization resulting in a kind of a macroscopic built-in internal bias field (like the high electric field applied at usual ferroelectric phase transitions). Another characteristic of this asymmetry is the local electrooptic loop measured at a certain point by sweeping the *dc* bias field (Fig. 4a), which is similar to the asymmetric tuning loops observed in ferroelectric thin films just near the local phase transition [8].

For comparison, similar local electrooptic loop measured in a PLTZN ceramic sample is presented in Fig. 4b. It shows relatively soft ferroelectric behavior with lower width and higher repeatability. The small asymmetry due to inhomogeneous internal built-in electric

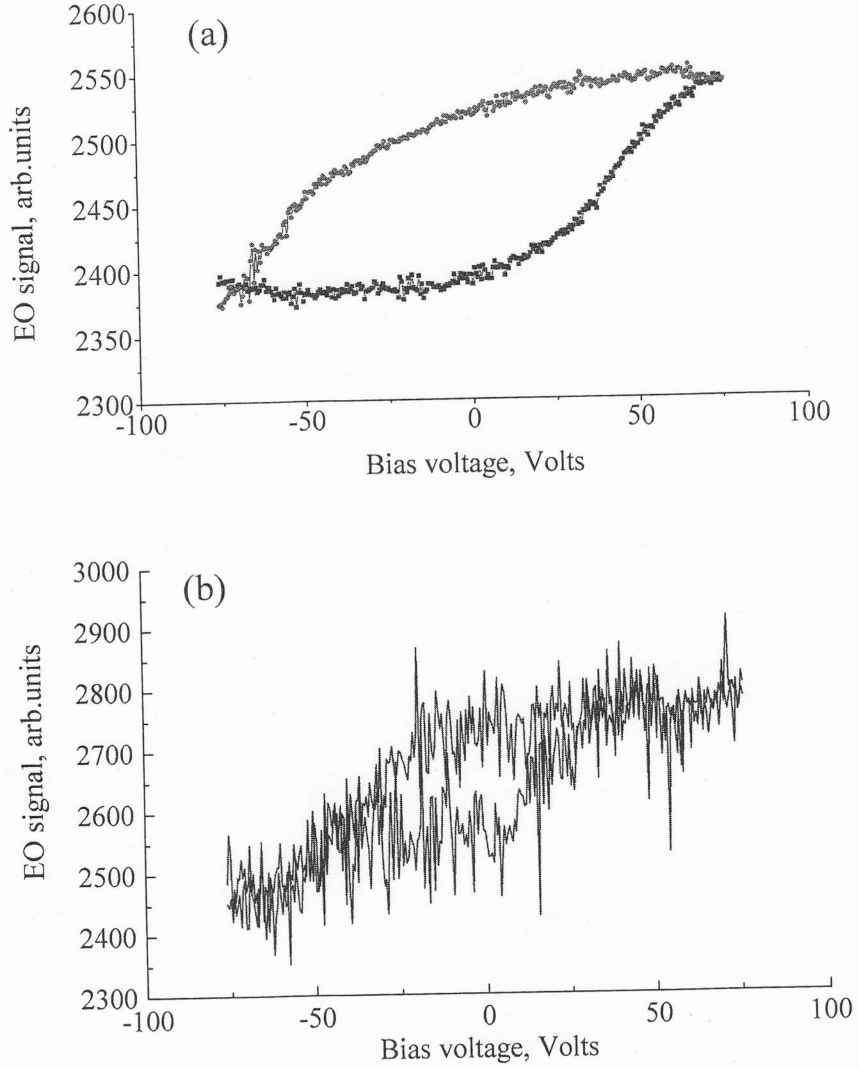

Figure 4. Local electrooptic loops in (a) PMN-PT crystal and (b) PLZNT ceramics.

fields still can be observed. However, this effect is less pronounced in PLZTN ceramics comparing to PMN-PT single crystals [13].

Difference between the two materials is even more evident in electrooptic images. Figure 5 shows a sequence of domain states in PLZTN during the variation of the *dc* bias voltage. Similar to PMN-PT, there are no microscopic domains in the virgin ceramic sample, and they appear irreversibly with application of a moderate electric field. Contrary to the stable domain structure in PMN-PT, most of the spatial regions change the sign of electrooptic response at the highest absolute values of the applied voltage (Fig. 5a, d), while intermediate stages of the switching process (corresponding to lower voltage) are characterized by reduced electrooptic contrast (Fig. 5b, e). This is an indirect confirmation of the fine intermediate structure of the real domains below the threshold of optical resolution.

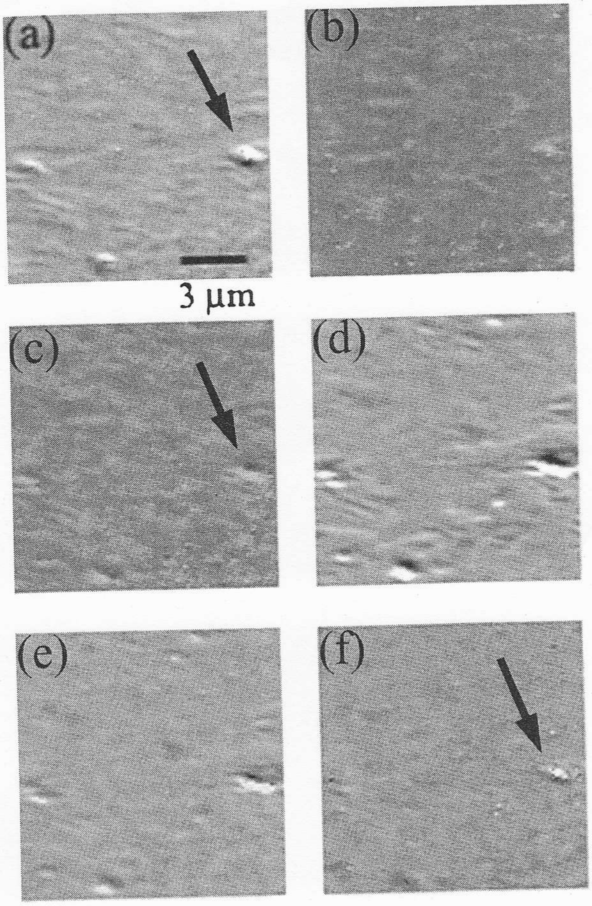

Figure 5. Evolution of the domain structure in PLZTN ceramics during application and variation of the *dc* bias voltage: (a) −100 V, (b) 0 V, (c) +35 V, (d) +100 V, (e) 0 V, (f) −70 V.

An interesting feature of electrooptic images of PLZTN ceramics is a bilateral change of the sign of the response induced by the *dc* bias field. If, for example, the field is changed from negative to positive (Fig. 5a–d), some regions change their color from dark to bright while other ones, inversely, from bright to dark. This is easy to see on the high contrast domain pairs like the one indicated by an arrow. Such behavior is not typical for more conventional imaging techniques, where the output signal tends to be homogeneous in high field (either dark or bright) depending on the field sign. This feature was neither observed in previous SEOM studies of ferroelectric single crystals [4].

Origin of this unusual contrast as well as other SEOM properties can be understood from the analysis of the electrooptic equation. For normal reflection from a crystallite of rhombohedral $3m$ symmetry the electrooptic response is proportional to:

$$\Delta(1/n^2) = \mathrm{r}_{\mathrm{ijk}} E_{\mathrm{k}} = r_{13}\cos\theta\sin^2\varphi + \mathrm{r}_{33} E\cos\theta\cos^2\varphi + 2\mathrm{r}_{51}\sin\theta\sin\varphi\cos\varphi, \qquad (1)$$

where $\mathrm{r}_{\mathrm{ijk}}$ – electrooptic tensor, n - optical index, E - applied sinusoidal electric probe field, and angles θ and φ describe deviation of the electric field and of the light polarization direction, respectively, from the ferroelectric c axis component in the plane of the surface

[3]. Reversal of the ferroelectric polarization results in shift of both angles θ and φ by 180°, and the *ac* signal changes its sign, but keeps the same absolute value. However, chaotic angular distribution of crystallographic axis, typical for ceramics, combined with continuous spectrum of angles between the field and local ferroelectric polarization, make non-180° switching possible and even common. In this case the phase of the electrooptic response is not anymore symmetric with respect to switching. It can be readily seen, for example, from Fig. 4b of Ref. [3]: even small variations of the angle θ can induce reversal of the electrooptic contrast, and both black-to-white and white-to-black signal changes can coexist at the same geometrical conditions. It is interesting to note that, for example, tetragonal barium titanate shows no such variety of possible electrooptic response (Fig. 6b of Ref. [3]) due to the fact that one component of the electrooptic tensor is much higher than the other ones. It means that, first, effect of the bilateral switching of the electrooptic contrast should not be observed in $BaTiO_3$ ceramics; second, the SEOM images of a ceramic material allow one to draw some conclusions about features of its electrooptic tensor even without any quantitative measurements.

In conclusion, we have applied scanning confocal electrooptic microscopy to visualize field-induced formation and evolution of microscopic domains in two relaxor materials – PMN-PT single crystals and PLZNT ceramics. Domains in PLZTN are more sensitive to the applied electric field, while those of PMN-PT are relatively stable, and local electrooptic loops in this material are relatively wide and non-symmetric, apparently due to strong internal field. The difference between electrooptic images of crystals with different orientation has been qualitatively explained on the basis of the electrooptic tensor analysis. Bilateral reversal of the electrooptic contrast in presence of the bias field has been observed and explained.

Acknowledgments

This research was supported by a *Marie Curie International Fellowship* within the 6th European Commission Framework Programme, contract MIF CT 2004 002557, and by the Fondazione Cassa di Risparmio di Pisa. We are grateful to Dr. Valeriy Smotrakov, Dr. Laurent Lebrun, and Dr. Carmen Galassi, who provided the samples for our studies.

References

1. W. J. Merz, *Phys. Rev.* **88**, 421 (1952).
2. C. Hubert, J. Levy, A. C. Carter, W. Chang, S. W. Kiechoefer, J. S. Horwitz, and D. B. Chrisey, *Appl. Phys. Lett.* **71**, 3353 (1997).
3. O. Tikhomirov, B. Red'kin, A. Trivelli, and J. Levy, *J. Appl. Phys.* **87**, 1932 (2000).
4. O. Tikhomirov and J. Levy, *Ferroelectrics* **292**, 161 (2003).
5. X. K. Orlik, M. Labardi, and M. Allegrini, *Appl. Phys. Lett.* **77**, 2042 (2000).
6. C. Hubert and J. Levy, *Appl. Phys. Lett.* **73**, 3229 (1998).
7. C. Hubert, J. Levy, T. V. Rivkin, C. Carlson, P. A. Parilla, J. D. Perkins, and D. S. Ginley, *Appl. Phys. Lett.* **79**, 2058 (2001).
8. O. Tikhomirov, H. Jiang, and J. Levy, *Appl. Phys. Lett.* **77**, 2048 (2000).
9. O. Tikhomirov, H. Jiang, and J. Levy, *Phys. Rev. Lett.* **89**, 147601 (2002).
10. O. Tikhomirov, M. Labardi, C. Ascoli, M. Allegrini, and L. Lebrun, (to be published).
11. F. Bai, J. Li, and D. Viehland, *J. Appl. Phys.* **97**, 054103 (2005).
12. X. Wan, H. Luo, X. Zhao, D. Y. Wang, H. L. W. Chan, and C. L. Choy, *Appl. Phys. Lett.* **85**, 5233 (2004).
13. O. Tikhomirov, M. Labardi, C. Ascoli, M. Allegrini, and C. Galassi, (to be published).